

Chapter 12

Machine Protection in the High Luminosity LHC

A. Apollonio^a, P. Bélanger^b, D. Carrillo^c, R. Denz^c, F. Rodriguez Mateos^c,
B. Panev^c, A. Siemko^c, J. Uythoven^c, A. Verweij^c, D. Wollmann^c and M. Zerlauth^d

^a*Former CERN member*

^b*CERN, BE Department, Genève 23, CH-1211, Switzerland*

^c*CERN, TE Department, Genève 23, CH-1211, Switzerland*

^d*CERN, ATS-DO Unit, Genève 23, CH-1211, Switzerland*

In the high luminosity era of the LHC, the energy stored in the two beams will nearly double as compared with the design value of the current LHC and the beta functions will significantly increase in critical locations. In addition, novel equipment like Nb₃Sn based superconducting magnets, crab cavities, hollow e-lenses and others will be installed. These changes require the careful review of known fast failure cases and the study of newly emerging ones. Furthermore, a new generation of magnet and circuit protection systems will be applied in the HL-LHC, which will set a new standard in this field. Finally, a high machine availability will be one of the key factors to achieve the challenging integrated luminosity goals of the HL-LHC era. Therefore, the overall availability targets in terms of the allowed number of beam dumps and fault recovery time are defined.

1. Introduction

In the high luminosity era of the LHC, the bunch intensity will nearly double as compared to the nominal LHC design and, therefore, the stored beam energy will increase to about 700 MJ in each of the two proton beams. At the same time, new accelerator equipment like Nb₃Sn based inner triplet superconducting magnets in IP1 and 5, 11 T dipole magnets for the dispersion

This is an open access article published by World Scientific Publishing Company. It is distributed under the terms of the Creative Commons Attribution 4.0 (CC BY) License.

suppressor regions of IP7, new superconducting separation and re-combination dipoles, as well as crab cavities, hollow e-lenses and other new equipment will be installed. Furthermore, the beta functions will increase at critical locations of the accelerator by up to a factor of four.¹ These changes require the careful review of already known and the study of newly emerging fast failure cases introduced by new equipment and technologies, to ensure that the existing machine protection system can safely abort the beams before damage to the experiments or accelerator equipment occurs. The results of these studies will be described in Section 2. Their impact on the required evolution and upgrades of the LHC interlock systems will be discussed in Section 3.

The protection of the new inner triplet circuits in IR1 and IR5, which are based on large aperture inner triplet Nb₃Sn quadrupole magnets depends on classical quench heaters and the novel coupling loss induced quench (CLIQ) protection system, new radiation tolerant cold power diodes and a newly developed, universal quench detection system (UQDS).¹ Furthermore, a new generation of energy extraction systems based on in-vacuum switches will be used for the protection of corrector circuits of the HL-LHC insertion magnets. The details of these next generation magnet and circuit protection systems will be discussed in Section 4. Section 5 will discuss the aspects of machine availability for the HL-LHC.

2. Fast Failures and Protection in the HL-LHC

In the following two subsections, the criticality of known fast failures resulting from the HL-LHC machine parameters and beam intensities will be summarized and new fast failures described. Finally, the expected impact of beam-dust interactions on HL-LHC performance will be described.

2.1. *Scaling of known fast failures to HL-LHC*

Injection and extraction failures are so-called ultra fast failures and the protection against them depends primarily on the use of passive protection elements. Due to the increase in bunch intensity and beam brightness some of these elements will require to be upgraded for HL-LHC.¹ The impact of particle showers from these protection elements into downstream superconducting magnets during such events has been studied, showing that the expected levels

of energy deposition of up to about 100 Jcm^{-3} in Nb-Ti based magnets are not critical. Degradation of the thermal stability of LHC type Nb-Ti superconductor strands was observed for energy depositions above 2 kJcm^{-3} , which is equivalent to hot-spot temperatures of 680 K. However, no degradation of the critical current density was observed after beam impacts with an energy deposition of about 4 kJcm^{-3} (equivalent to a hot-spot temperature of about 1200 K) in LHC type Nb-Ti strands.²

The normal conducting separation dipoles (D1) in IP1 and IP5 will be replaced by superconducting magnets. Therefore, the very fast impact on the beam due to a powering failure³ in these circuits will be mitigated due to the significantly increased circuit discharge time constants. In case of a quench or another failure in the powering of the new RD1 circuits, the beam dump will be initiated via the Powering Interlock Controller (PIC) and Beam Interlock System (BIS).

The impact of the coherent beam-beam kick on the HL-LHC has been studied and discussed in.⁴ Recently, these results have been reviewed based on simulation models bench-marked with measurement data from LHC Run 2. The results show that a significant orbit distortion of up to 1.6σ has to be expected in the second turn after a sudden loss of the coherent beam-beam kick in HL-LHC.⁵ For this reason, a hardware linking of the beam permits of the two beams at the level of the Beam Interlock System is required for high intensity operation, ensuring that the delay between the dumping of the two beams is limited to a maximum of one turn.

The LHC transverse damper (ADT) can, besides its main functionality of damping, also be used to coherently excite the full beam or parts of it. At its maximum voltage of 7.5 kV, beam losses will reach critical levels after only 10 turns.⁵ This is sufficient for the beam loss monitors (BLMs) and the beam current change monitor (BCCM) to interlock on beam losses. However, the maximum deflecting voltage of the ADT should not be increased beyond the current value and the functionality of coherently exciting the beam should be limited to only a fraction of the full beam, e.g. 144 bunches, to gain margin between the time of interlocking and reaching critical loss levels. The effect of a partially depleted beam halo due to the use of the hollow e-lens on this time margin must be carefully studied.

A fast symmetric quench of one of the triplet magnets in IP1 has been observed in LHC Run 2. This quench caused a beam dump due to beam losses

after 242 turns. With the significantly increased beta functions in the triplets of IP1 and IP5 during the HL-LHC era, critical levels of orbit excursion due to a similar event could be reached after only about 55 turns.⁵ In such an event, the protection against excessive beam losses entirely depends on the BLMs and the BCCM, as the intrinsic delays of the quench detection system are longer. The criticality of these types of events needs to be reviewed in case of significant changes to the beam optics or the interlock thresholds in the future. Furthermore, the effect of a partial depletion of the beam halo on the protection in case of such an event has to be studied carefully.

2.2. Fast failures related to new equipment

Following a beam induced quench in one of the LHC main dipole magnets, a periodic loss pattern in the LHC collimation region was observed. These losses were traced back to an orbit excursion caused by the skew dipole kick induced on the beam by the firing of the quench heaters of the concerned main dipole.⁶ This observation triggered a detailed study of the expected effects of magnet and circuit protection elements like quench heaters and the novel CLIQ systems⁷ on the circulating beam of HL-LHC. As a result, the connection schemes for quench heater circuits in the new HL-LHC triplet, D1 and D2 magnets as well as the connection scheme of the CLIQ systems in the triplet circuits have been revised to reduce their impact on the circulating beam in a way which is coherent with protection requirements of the superconducting circuits.^{5,6} However, the effects of a spurious discharge of a quench heater in one of the triplet magnets and the D1 as well as a spurious discharge of a CLIQ unit in one of the triplet circuits, would still lead quickly to critical beam excursions. Therefore, the spurious discharges of the quench heaters of these magnets as well as of CLIQ systems have to be interlocked during HL-LHC operation and the extraction of the beams must be ensured within ten turns.⁵

During the first test of crab cavities with proton beams in CERN's Super Proton Synchrotron (SPS) in 2018⁸ dedicated machine protection tests were performed, confirming previously studied failure cases.⁹ The most critical failure case observed was due to resonant beam excitation, when the crab cavity phase crossed the betatron tune.¹⁰ This confirms the need for a fast interlock of the crab cavity voltage and phase in HL-LHC.

2.3. Beam-dust interactions

Micrometer-sized dust particulates, made of fine grains of solid matter, are known to have caused intensity drops in electron storage rings (TRISTAN, CESR, HERA, DORIS),^{11–13} pressure bursts in the SuperKEKB positron storage ring¹⁴ and sporadic beam losses as well as magnet quenches in the LHC.^{15–17} The presence of dust contamination in the vacuum chamber of the LHC is not fully understood and seems unavoidable, even with careful cleaning measures.¹⁸ As a result, the same phenomenon is expected to occur in the HL-LHC.

Dust sampling carried out in the vacuum system of the LHC revealed the presence of grains of different materials, with radii ranging from 1 μm to 200 μm . Experimental observations suggest that this dust was introduced during the assembly of the LHC.¹⁹ During operation, dust grains can become charged due to both electron clouds and synchrotron radiation.²⁰ Negatively charged grains are attracted by the beam of the LHC, get ionized by the passage of the high energy protons and are eventually repelled out of the beam. The inelastic interactions of the beam with dust are significant enough so that the resulting beam losses risk triggering the interlock systems and cause magnet quenches. For historical reasons, beam-dust interactions in the LHC are commonly referred to as Unidentified Falling Objects, or UFOs. Throughout LHC Run 1 and Run 2, UFOs were observed sporadically all around the LHC, with no clear source or triggering mechanism. Typical beam losses follow an asymmetric Gaussian profile lasting up to a few milliseconds, with integrated doses between 10^{-7} Gy and 10^{-3} Gy. The main mitigation strategy used to reduce the impact of UFOs was to increase the threshold of certain Beam Loss Monitors (ICBLMs) towards or above the assumed magnet quench limit¹⁶ and to profit from the conditioning effect of high intensity beam operation.²¹

The dynamics of UFOs is mainly driven by the charge-to-mass ratio of the grain, which depends on the ionization rate following the interaction with the beam. On that matter, simulations are in good agreement with measurements and indicate that UFOs must carry an initial negative charge before the interaction with the beam.²² Based on these results, UFO time profiles recorded by the LHC BLMs have been used to narrow down the size and charge distribution of the dust grains which interacted with the LHC beam during Run 2.²³ Moreover, a theoretical model for the charging mechanisms

at play in the beam pipe of the LHC was developed²⁰ and is consistent with the expected charge. However, the triggering mechanism of UFO events is still not understood and remains the main unknown related to the UFO phenomenon, in particular the sporadic release of UFOs around the LHC ring.

3. Interlocks

The machine protection of the HL-LHC will be based on the existing interlock systems already present for the LHC. The core systems related to HL-LHC are the Beam Interlock System (BIS) with the Safe Machine Parameter (SMP) system and the Power Interlock Controller (PIC) for the protection of the superconducting magnets. These three systems will have a consolidation upgrade foreseen for Long Shutdown 3, which allows for making some system changes taking into account new HL-LHC requirements.

The reaction time of the BIS is determined by the physical transmission time of the beam permit signals through optical fibres around the LHC circumference. As there is no clear requirement to have a faster beam abort, the optical infrastructure of the BIS will not be changed. The only change of the system will be the hardware linking of the beam permit signals of the two beams above a certain beam intensity. This will very likely be introduced with the implementation of an additional flag of the SMP system.

The operational limits of the passive beam absorbers (TCDQ, TCDS, TDIS) mainly depend on the intensity of a few bunches hitting these absorbers in the case of acceptable failure scenarios related to the injection or beam abort process. To obtain flexibility in interlocking and machine operation, the new SMP system will produce one or several additional flags related to the maximum bunch intensity.

Many new HL-LHC elements are important and even critical for machine protection, due to the failure modes identified in the section above. For this reason, systems like the crab cavities, will be connected to the BIS as additional interlocks. The hollow electron lens will be connected to the PIC, related to the protection of its superconducting circuits, and by this also to the BIS. A direct link between the hollow electron lens system and the BIS could be required to abort the beam, depending on the operating conditions. In this context, a link between the coronagraph and BIS can also be envisaged.

For the HL-LHC operation with increased beam intensities some areas where the BIS user connections (CIBUs) are located have been identified as requiring radiation tolerant electronics. Also the PIC equipment in the RRs will see larger radiation doses and the new electronics developed for both the CIBUs and part of the PIC electronics will be made radiation tolerant.

4. Circuit Protection

The various superconducting circuits for the HL-LHC (see also Chapter 9) will be protected against overheating due to quenches in several ways, relying on either self-protection, energy extraction, quench heaters, or a combination of quench heaters and CLIQ. Quench detection systems are implemented on all circuits except for some higher-order corrector circuits which rely on self-protection. All quench detection and protection systems are built from robust and reliable components to minimize the risk of overheating and possible degradation of the magnet performance. Realistic failure scenarios are taken into account, and sufficient redundancy in the quench detection and protection systems is implemented to cope with these failure scenarios.

The triplet circuit consists of a series of six quadrupole magnets (Q1a/b, Q2a/b, Q3a/b) powered by a main converter, two 2 kA trim converters, and one 35 A trim converter on the Q1a. Each quadrupole magnet contains eight quench heater circuits and is connected to one CLIQ unit. In case of a quench in any superconducting part of the circuit (magnet, busbar, current lead), the power converters will be switched off and all 48 quench heaters and six CLIQ units are fired, hence quickly discharging the circuit current and depositing the stored energy rather uniformly in the coils of the six quadrupole magnets.

The quench protection of the D1 and D2 magnet circuits relies on eight quench heaters connected in four electrical circuits. The D2 magnet contains as well eight spare quench heaters. In case of a quench in the superconducting magnet, busbar or current lead, the power converter will be switched off and all eight quench heaters are fired. The fast increase of the coil resistance ensures a discharge of the circuit current with a pseudo-time constant of about 0.4 s at nominal current.

The quench protection of the orbit corrector circuits in the inner triplet relies on external energy extraction. In case of a quench in the superconducting magnet, busbar or current lead, the power converter will be switched off and

the energy extraction switch will be activated, hence including an external dump resistor in the circuit. The fast discharge of the circuit current with a pseudo-time constant of about 0.4 s to 1.5 s, depending on the circuit, will ensure sufficient margin for the maximum temperature of the coil and the maximum voltage to ground.

Also the quench protection of the D2 orbit corrector circuit and the quench protection of the inner triplet skew quadrupole corrector circuit rely on external energy extraction. In case of a quench, the power converter will be switched off and the energy extraction switch will be activated, similar to the triplet orbit corrector circuits, hence dissipating most of the magnet stored energy in a dump resistor.

The higher order triplet corrector circuits covering, sextupole, octupole, decapole and dodecapole magnets are all self-protected. In case of a quench in any of the magnets of these circuits, the power converter will shut down and the quench propagation in the coils will generate sufficient resistance to discharge the current fast enough to avoid overheating of the coil. The busbars of these circuits are cryostable.

4.1. Energy extraction systems

The HL-LHC requires the introduction of 44 new energy extraction (EE) systems for protection of the new superconducting triplet and triplet orbit corrector and triplet skew quadrupole circuits. Two classes of systems, one for 600 A and another one for 2 kA have been developed to cover the HL-LHC requirements. The new EE systems introduce a novel DC switching technology, the DC in-vacuum switches, in the quench protection equipment and provide some essential features such as an ultra-fast switch opening, less maintenance and long service life operation.

The energy extraction systems use off-the-shelf in-vacuum interrupters as a switching element. To ensure high-speed reaction during opening, each interrupter is activated by an inductive-dynamic driver (IDD) mechanism based on the Thompson coil principle. The classical configuration of two redundant switches connected in series and controlled simultaneously is implemented for each system. To rupture the circuit current and extinguish the following electrical arc, the in-vacuum switches use a so-called forced commutation method. This technique is based on a strong counter-current pulse gener-

ated during the switch opening process which makes the main current in the vacuum chamber to cross zero and complete the commutation. Pre-charged capacitors controlled through thyristor switches are the sources for the IDD and counter-current auxiliary circuits. Each in-vacuum switch is a single-pole, bipolar device, built in a sliding cassette to facilitate its replacement if necessary, and connected to the power part through flexible bus bars. The power part structure is sized according to the specified current density of 1.6 A/mm^2 . A simple and reliable locking device ensures the opening status when the contact of the interrupter is opened. Optical fibers provide galvanic separation and fast links for trigger signals and digital readouts. For redundancy, two auxiliary low-voltage power supplies with status supervision are used. The switch control unit is using the IGLOO2, flash-based FPGA platform from Microsemi-Microchip to control the operation of the switch. All safety-critical signals and interlocks are redundant.

Dump resistors are custom-made, high-temperature wire wound resistors produced in industry. There are four, permanently connected in a redundant configuration, to ensure the proper resistance level and safe operation in case of a failure in one of them. The resistors are equipped with temperature sensors and thermal switches for supervision.



Fig. 1. In-vacuum switch based 2 kA energy extraction system.

The in-vacuum switch EE systems are integrated in a standard EURO rack with dimensions $600 \times 900 \times 2000$ (see Figure 1). Each 2 kA system is housed in one rack while for the 600 A version, two EE systems share one rack. The power terminals, at the top of the racks fulfil the IP20 norm.

4.2. Coupling loss induced quench systems

The coupling loss induced quench (CLIQ) system is an innovative technology for the protection of superconducting magnets in case of a quench.⁷ Its fast and effective heating mechanism, utilizing coupling losses, and its robust electrical design makes it a very attractive solution for high-field magnets. The CLIQ technology has been successfully applied to magnets of different sizes, coil geometries and types of superconductor.

The CLIQ system is composed of a capacitor bank C, a floating voltage supply S, two resistive current leads CL1 and CL2 connecting the system to the magnet, and a Bidirectional Controlled Thyristor (BCT) package, indicated as TH in Figure 2.

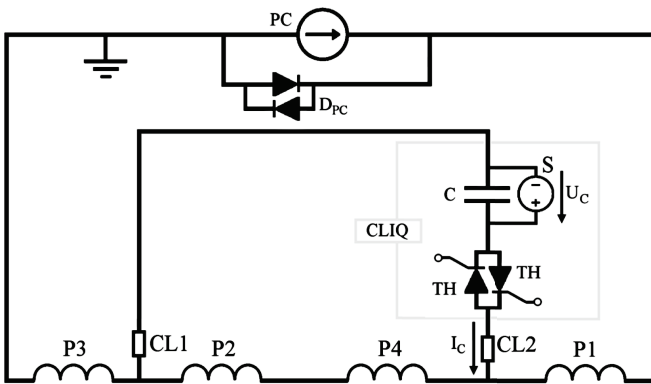


Fig. 2. Schematics of a CLIQ system connected to protect a superconducting magnet.⁷

The capacitor bank is charged by S with a voltage U_C . Upon quench detection, the thyristors are activated resulting in a current I_C discharging through CL2 causing an over-current in magnet poles P2-P4 and an under-current in magnet poles P1-P3 as compared to the nominal current in the magnet as shown in Figure 3.

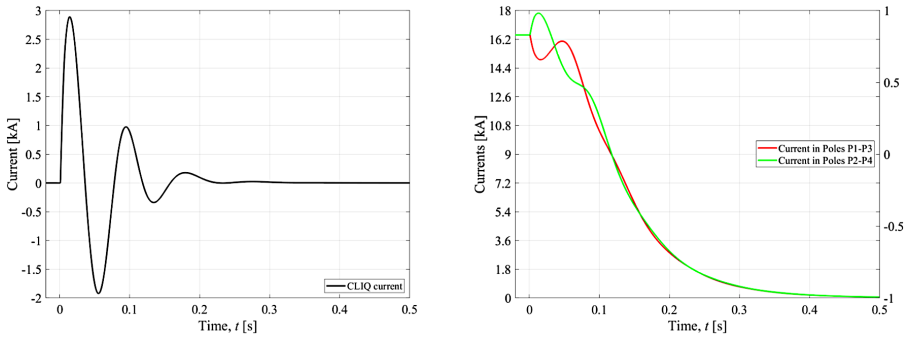


Fig. 3. Oscillation of the CLIQ current I_C (left) and current in the poles of the magnet (right) following the activation of the CLIQ thyristor as simulated with STEAM-LEDET.^{24,25}

So far eleven CLIQ units of industrial-grade have been manufactured and successfully qualified.²⁶ Compared to these, the HL-LHC version will include an improved monitoring system, enhanced electronics and a higher reliability configuration. As core component, each unit will contain a polypropylene film capacitor bank with a total capacitance of 40 mF and nominal operating voltage of 1 kV, hence discharging an energy of approximately 20 kJ into the connected magnet. Figure 4 shows units of the second generation prototypes, manufactured for the tests of prototype magnets.



Fig. 4. CLIQ prototype units of the second generation at the test lab.

4.3. Quench heater power supplies

The quench heater discharge power supplies (QHDS) are the units responsible for energizing the quench heater strips in order to dissipate the energy stored in the magnet into its full volume, hence limiting the hot-spot temperature at the location of the original quench and preventing damage to the coil. Every QHDS consists of a capacitor bank with six aluminium electrolytic capacitors arranged in two sets of three capacitors each. These are connected in series, providing a total capacitance of 7.05 mF. Figure 5 shows a simplified scheme of a QHDS.

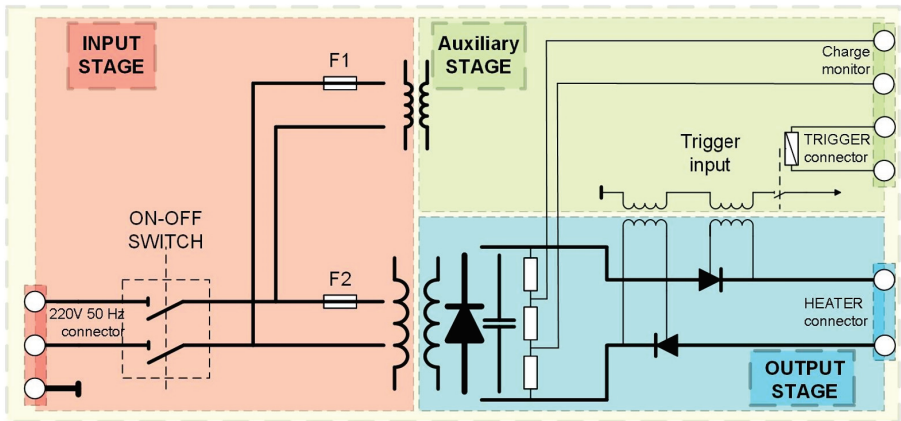


Fig. 5. Simplified electrical scheme of a QHDS unit.

The nominal operating voltage of the capacitors will be 450 V and therefore an overall voltage for the capacitor bank of 900 V is expected to deliver ~ 3 kJ to a single quench heater strip when the unit is triggered by the quench detection system.

Presently, there are over 6000 QHDS installed in the LHC and additional 256 QHDS with improved capabilities and higher reliability will be needed for HL-LHC in order to protect the 11 T dipoles (MBH), the inner triplet magnets in IP1 and IP5 as well as the new separation and re-combination dipoles D1 and D2. Figure 6 shows one QHDS for the protection of the 11 T dipole (MBH).



Fig. 6. QHDS for the protection of the 11 T dipole (MBH) magnets.

4.4. Cold diodes

Cold power diodes are an essential part of the protection of the new HL-LHC triplet circuits in IP1 and 5. Their role is to contain voltage and current transients within the cold part of the circuit without transmitting those effects to the superconducting link and the warm elements. Furthermore, they protect the triplet magnets from excessive quench voltages in case of a non-uniform distribution of the resistance in the magnet coils. The cold diodes will be placed in the so-called DCM, a cryostat connecting module which will be installed close to the separation dipole D1. In this position, they will be exposed to high levels of radiation from the interaction point. The expected integrated dose and fluence levels at their position by the end of life are 12 kGy and $5 \times 10^{13} \text{ cm}^{-2}$ in 1 MeV neutron equivalent (n-eq) units.²⁷

Three types of power diodes with different n-base widths were irradiated at cryogenic temperatures up to a 1 MeV n-eq fluence of $2.2 \times 10^{14} \text{ cm}^{-2}$ and 12 kGy in CERN's CHARM facility.²⁸ The forward voltage increased between approximately 43% for the diodes with very thin n-base width to about 83% for the LHC reference diode type at the end of the irradiation campaign when compared to the initial values. Partial annealing of the radiation damage has been observed after a thermal cycle to room temperature. Due to this effect, the increase of the forward voltage due to radiation damage after annealing was close to halved in all three diode types.^{2,29}

Although all three types of diodes were fulfilling the specifications for the protection of the HL-LHC triplet circuit at the end of the irradiation campaign, the most radiation tolerant (very thin n-base width) diode type was

chosen for the series production. This, together with the possibility of partial annealing through a thermal cycle, provides comfortable margin within the uncertainty of the expected integrated dose and fluence levels at the end of life of the triplet circuit.

4.5. Quench detection system

The protection and diagnostics of the new HL-LHC magnets and circuit elements require the development of a new generation of integrated quench detection and data acquisition systems (QDS). For the HL-LHC QDS a unified approach, the Universal Quench Detection System (UQDS), has been proposed³⁰ and several prototypes have been built (see Figure 7).



Fig. 7. UQDS v2.1 crate serving as the baseline prototype for the 11 T dipole (MBH) quench detection system. The crate is not equipped with top covers to illustrate its construction.

4.5.1. UQDS general architecture

As a flexible and generic system, the UQDS architecture is not connected to a specific quench detection algorithm and can be configured according to the requirements of the protected superconducting element. In case of the HL-LHC, the UQDS can be adapted to the needs of various magnet technologies and provide as well efficient protection for the novel MgB_2 high current cable links. One of the key elements of the UQDS architecture are the analogue front-end channels equipped with a high-resolution analogue-to-digital converter (ADC) of the successive approximation type. Insulated DC-DC converters and digital isolators for the serial data interfaces provide galvanic isolation of the analogue channels. In the foreseen implementation up to 16 of such channels connect to a field programmable gate array (FPGA), which processes

the acquired data and executes the quench detection algorithms. To enhance reliability UQDS units are always deployed as a set of two independent units reading signals from two redundant sets of instrumentation voltage taps. Each unit is powered by two independently monitored power supply units. The UQDS units are equipped with dedicated hardware interlocks for the activation of the protection elements of the magnet circuit such as quench heater discharge power supplies, coupling loss induced quench systems and energy extraction systems. The built-in field-bus interface provides the data link to the front-end computers of the accelerator control system.

5. Availability Aspects

Operating HL-LHC with high availability will be one of the key factors to achieve the challenging integrated luminosity goals of the HL-LHC project. The target production is set to 250 fb⁻¹ over 160 days of operation per year, which implies an average daily production of 1.56 fb⁻¹. Considering the latest reference beam parameters,¹ a HL-LHC fill colliding for 12 h (with 7.2 h levelling time) produces about 1.8 fb⁻¹. This allows setting a high-level goal for HL-LHC physics efficiency (i.e. fraction of time in collisions) of 50%, including some margin. Such a goal is in line with LHC performances during Run 2, which reported a physics efficiency of 49% in the years 2016-2017-2018. Nevertheless, a number of factors will make achieving this goal a challenge for HL-LHC. The beam energy will be 7 TeV, potentially affecting availability for what concerns the number of magnet flat-top quenches (or ‘de-training’ quenches) and beam-induced quenches (mainly induced by UFOs, see section 2.3 of this Chapter). In addition, the energy increase implies that many systems will be operated closer to their design limits. The beam dumping system in particular, whose failure rate is known to depend on the operating energy, has undergone major consolidations during LS2, which should reduce its sensitivity to higher operating voltage. Failure rates for the new system will have to be re-assessed during LHC Run 3. Thanks to available margins, it is estimated that the failure rate of power converters will not be significantly affected. In general, failures of electronics due to radiation are not expected to be a major limitation to operation, thanks to the dedicated radiation tolerant designs developed in view of the HL-LHC era, which will allow coping with increased fluences. The cryogenic system will

have to cope with increased heat loads without significantly affecting availability. The deployment of additional cryoplants in points 1 and 5 inevitably implies a higher failure rate for the system. In addition, in order to reach the set integrated luminosity goal, the performance of new HL-LHC systems (crab cavities, superconducting link, Nb₃Sn magnets) will have to be in line with the performance of present LHC systems. Back-up mitigation strategies should be defined in case of significant performance loss due to any of the new systems (e.g. use of flat optics as a back-up for the use of crab cavities). In the HL-LHC era the role of the injectors will already be of even higher importance than for today's LHC. Extended operation with levelling implies shorter optimal fill lengths than for LHC, which requires performing more machine cycles and, thus, more injections. Even with lower demand rates experienced in LHC Run 2, the injector complex has been the first contributor to LHC unavailability. Optimizing the injection process for HL-LHC beams will be a key aspect for achieving the target physics efficiency. LHC Run 3 will already offer the possibility to achieve this thanks to the production of higher brightness beams made possible by the LHC Injectors Upgrade. Figure 8 allows defining the overall availability targets for these systems in terms of number of allowed beam dumps and fault recovery time.

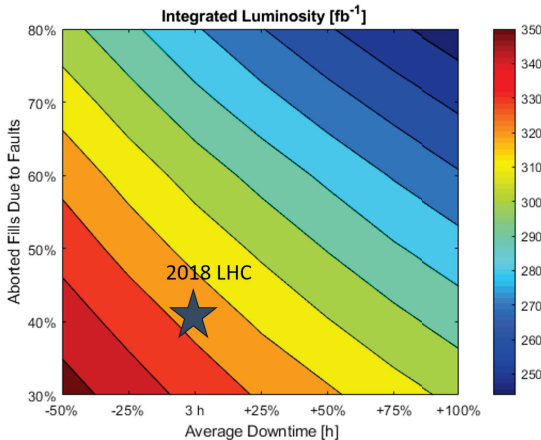


Fig. 8. HL-LHC Integrated luminosity production as a function of average downtime and number of aborted fills due to faults. The star indicates the yearly luminosity production expected in the HL-LHC era, if the HL-LHC will achieve a similar machine availability as the LHC in 2018.

References

1. I Béjar Alonso, O Brüning, P Fessia, L Rossi, L Tavian, and M Zerlauth. *High-Luminosity Large Hadron Collider (HL-LHC): Technical design report*. CERN Yellow Reports: Monographs. CERN, Geneva, 2020.
2. Andreas Will. Damage mechanisms in superconductors due to the impact of high energy proton beams and radiation tolerance of cryogenic diodes used in particle accelerator magnet systems, 2021. Presented on 23 April 2021, to be published.
3. B Goddard, V Kain, R Schmidt, and M Zerlauth. Detecting Failures in Electrical Circuits Leading to Very Fast Beams Losses in the LHC. (LHC-Project-Report-749. CERN-LHC-Project-Report-749):4 p, 2004. revised version submitted on 2004-09-23 10:55:35.
4. Tobias Baer. Very Fast Losses of the Circulating LHC Beam, their Mitigation and Machine Protection, Oct 2013. CERN-THESIS-2013-233.
5. B. Lindstrom, P. Bélanger, L. Bortot, R. Denz, M. Mentink, E. Ravaoli, F. Rodriguez Mateos, R. Schmidt, J. Uythoven, M. Valette, A. Verweij, C. Wiesner, D. Wollmann, and M. Zerlauth. Fast failures in the lhc and the future high luminosity lhc. *Phys. Rev. Accel. Beams*, 23:081001, Aug 2020.
6. Matthieu Valette, Lorenzo Bortot, Alejandro Fernandez Navarro, Bjorn Lindstrom, Matthijs Mentink, Emmanuele Ravaoli, Ruediger Schmidt, Edvard Stubberud, Arjan Verweij, and Daniel Wollmann. Impact of Superconducting Magnet Protection Equipment on the Circulating Beam in HL-LHC. *Proceedings of the 9th Int. Particle Accelerator Conf.*, IPAC2018, 2018.
7. Emmanuele Ravaoli. CLIQ. A new quench protection technology for superconducting magnets, 2015. CERN-THESIS-2015-091.
8. R. Calaga, O. Capatina, and G. Vandoni. The sps tests of the hl-lhc crab cavities. In *Proc. 9th Int. Particle Accelerator Conf. (IPAC'18)*, pages 846–849. JACoW Publishing.
9. Andrea Santamaria Garcia. Experiment and Machine Protection from Fast Losses caused by Crab Cavities in the High Luminosity LHC, 2018. CERN-THESIS-2018-142.
10. B Lindstrom, H Bartosik, T Bohl, A Butterworth, R Calaga, L R Carver, V Kain, T E Levens, G Papotti, R Secondo, J Uythoven, M Valette, G Vandoni, J Wenninger, D Wollmann, and M Zerlauth. Machine protection experience from beam tests with crab cavity prototypes in the CERN SPS. *Journal of Physics: Conference Series*, 1350:012004, nov 2019.
11. Hiroshi Saeki, Takashi Momose, and Hajime Ishimaru. Observations of dust trapping phenomena in the TRISTAN accumulation ring and a study of dust removal in a beam chamber. *Review of Scientific Instruments*, 62(4):874–885, 1991.
12. David Sagan. Mass and charge measurement of trapped dust in the CESR storage ring. *Nuclear Instruments and Methods in Physics Research*, 330:371–379, 1993.
13. F Zimmermann. Trapped Dust in HERA and DORIS, 1993.
14. S Terui, Y Suetsugu, T Ishibashi, M Shirai, K Shibata, K Kanazawa, and H Hisamatsu. Observation of Pressure Bursts in the SuperKEKB Positron Ring. *Proceedings of IPAC 2018*, 2018.

15. G. Papotti, M. Albert, B. Auchmann, E. B. Holzer, M. Kalliokoski, and A. Lechner. Macroparticle-induced losses during 6.5 TeV LHC operation. *Proceedings of IPAC 2016*, pages 1481–1484, 2016.
16. T. Baer, M. J. Barnes, F. Cerutti, A. Ferrari, N. Garrel, B. Goddard, E. B. Holzer, S. Jackson, A. Lechner, V. Mertens, M. Misiowiec, E. Nebot Del Busto, A. Nordt, J. Uythoven, V. Vlachoudis, J. Wenninger, C. Zamantzas, F. Zimmermann, and N. Fuster Martinez. UFOs in the LHC: Observations, studies and extrapolations. *Proceedings of IPAC 2012*, 2012.
17. B. Goddard, P. Adraktas, T. Baer, M. J. Barnes, F. Cerutti, A. Ferrari, N. Garrel, A. Gerardin, M. Guinchard, A. Lechner, A. Masi, V. Mertens, R. Morón Ballester, S. Redaelli, J. Uythoven, V. Vlachoudis, and F. Zimmermann. Transient beam losses in the LHC injection kickers from micron scale dust particles. *Proceedings of IPAC 2012*, 2012.
18. B. Auchmann, J. Ghini, L. Grob, G. Ladarola, A. Lechner, and G. Papotti. How to survive a UFO attack. *Proceedings of the 6th Evian Workshop*, pages 81–86, 2015.
19. P. Bélanger. Unidentified falling objects in the large hadron collider: formation, charging mechanisms and dynamics of dust particulates in a high energy proton accelerator. Master's thesis, University of British Columbia, 2020.
20. P. Bélanger, R. Baartman, A. Lechner, B. Lindstrom, R. Schmidt, and D. Wollmann. Charging mechanisms and orbital dynamics of charged dust grains in the lhc. *Phys. Rev. Accel. Beams*, 2021. to be submitted.
21. A Lechner, M Albert, B Auchmann, C Bahamonde Castro, L Grob, E B Holzer, J Jowett, M Kalliokoski, S Le Naour, A Lunt, A Mereghetti, G Papotti, R Schmidt, R Veness, A Verweij, G Willering, D Wollmann, C Xu, and M Zerlauth. Blm thresholds and ufos. In *Proceedings of the 7th Evian Workshop on LHC Beam Operation, Evian Les Bains, France*, pages 209–214, 2016.
22. B. Lindstrom, P. Bélanger, A. Gorzawski, J. Kral, A. Lechner, B. Salvachua, and Others. Dynamics of the interaction of dust particles with the LHC beam. *Physical Review Accelerators and Beams*, 23(124501), 2020.
23. A. Lechner, P. Bélanger, B. Lindstrom, R. Schmidt, and D. Wollmann. Characteristics of dust- induced beam losses in the cryogenic arc sectors of the CERN Large Hadron Collider. *to be submitted to PRAB*.
24. Lorenzo Bortot, Bernhard Auchmann, I Cortes Garcia, AM Fernandez Navarro, Michał Maciejewski, Matthias Mentink, Marco Prioli, Emmanuele Ravaioli, S Schps, and AP Verweij. Steam: A hierarchical cosimulation framework for superconducting accelerator magnet circuits. *IEEE Transactions on applied superconductivity*, 28(3):1–6, 2017.
25. E. Ravaioli, B. Auchmann, M. Maciejewski, H. H. J. ten Kate, and A. P. Verweij. Lumped-Element Dynamic Electro-Thermal model of a superconducting magnet. *Cryogenics*, 80:346–356, 2016.
26. Felix Rodriguez-Mateos, David Carrillo, Stavroula Balampekou, Knud Dahlerup-Petersen, Mathieu Favre, Joaquim Mourao, and Bozhidar Panev. Design and Manufacturing of the First Industrial-Grade CLIQ Units for the Protection of Superconducting Magnets for the High-Luminosity LHC Project at CERN. Design and Manufacturing of the First Industrial-

- Grade CLIQ Units for the Protection of Superconducting Magnets for the High-Luminosity LHC Project at CERN. *IEEE Trans. Appl. Supercond.*, 28(3):4702504. 4 p, 2018.
27. R. García Alía, M. Brugger, F. Cerutti, S. Danzeca, A. Ferrari, S. Gilardoni, Y. Kadi, M. Kastriotou, A. Lechner, C. Martinella, O. Stein, Y. Thurel, A. Tsinganis, and S. Uznanski. Lhc and hl-lhc: Present and future radiation environment in the high-luminosity collision points and rha implications. *IEEE Transactions on Nuclear Science*, 65(1):448–456, 2018.
 28. Adam Thornton. CHARM Facility Test Area Radiation Field Description. Apr 2016.
 29. Andreas Will, G. D’Angelo, R. Denz, D. Hagedorn, A. Monteuis, E. Ravaoli, F. Rodriguez Mateos, A. Siemko, K. Stachon, A. Verweij, D. Wollmann, A.-S. Mueller, and A. Bernhard. Characterization of the radiation tolerance of cryogenic diodes for the high luminosity lhc inner triplet circuit. *Phys. Rev. Accel. Beams*, 23:053502, May 2020.
 30. Reiner Denz, Ernesto de Matteis, Andrzej Siemko, and Jens Steckert. Next Generation of Quench Detection Systems for the High-Luminosity Upgrade of the LHC. *IEEE Trans. Appl. Supercond.*, 27(4):4700204, 2017.